

General Disclaimer

One or more of the Following Statements may affect this Document

- This document has been reproduced from the best copy furnished by the organizational source. It is being released in the interest of making available as much information as possible.
- This document may contain data, which exceeds the sheet parameters. It was furnished in this condition by the organizational source and is the best copy available.
- This document may contain tone-on-tone or color graphs, charts and/or pictures, which have been reproduced in black and white.
- This document is paginated as submitted by the original source.
- Portions of this document are not fully legible due to the historical nature of some of the material. However, it is the best reproduction available from the original submission.

THE EFFICIENT CALCULATION OF THE TRANSPORT PROPERTIES
OF A DILUTE GAS TO A PRESCRIBED ACCURACY¹

by

H. O'Hara and Francis J. Smith
School of Physics and Applied Mathematics,
The Queen's University of Belfast,
Belfast, Northern Ireland.

No. of pages 25 + iii
No. of tables 4
No. of figures 4

¹This work was supported by the National Aeronautics and
Space Administration under Contract NSR-52-112-002 .

N69-32948

FACILITY FORM 602

(ACCESSION NUMBER)	(THRU)
33	1
(PAGES)	(CODE)
103701	19
(NASA CR OR TMX OR AD NUMBER)	(CATEGORY)

Correspondence to be sent to:

Dr. F.J. Smith,
Department of Applied Mathematics and Theoretical Physics,
The Queen's University of Belfast,
Belfast, BT7 1NN, Northern Ireland.

Running head

Transport Calculations

Abstract

We study in detail the numerical techniques needed to minimize the computation time in calculations of the transport properties of a dilute gas. We iterate all numerical processes until the results are uniformly correct to the accuracy prescribed by the user. Thus in 1 minute we may calculate a set of transport properties to an accuracy 1 in 100, but 10 minutes may be needed for an accuracy 1 in 10,000.

The principal numerical difficulties encountered are centred around the evaluation of some singular definite integrals. We eliminate the singularities by changes of variable and evaluate the resulting well behaved integrals using the Clenshaw-Curtis method. We found this to be the most efficient quadrature method mainly because of its accuracy and its error estimates. For the same reasons we adopted Chebyshev polynomial curve fitting techniques for interpolation rather than Lagrangian or Spline method.

I. Introduction

In the Chapman-Enskog theory [1] of a dilute gas the transport properties of the gas can be expressed in terms of a set of collision integrals $\Omega^{(l,s)}(T)$. These are functions of the temperature T and they depend on the interaction potentials between the atoms or molecules in the gas. A number of successful methods for calculating these collision integrals have been described in the literature [2-8] but we believe that the method we describe here is: (1) considerably more efficient than anything previously published; and (2) more reliable because we check the accuracy of every step in the calculation. It is also easier to use, takes up less storage space and the facility enabling the user to specify the accuracy which he needs should save him a great deal of computer time, especially in cases when he does not need great accuracy. The program is so fast that it is possible to calculate a set of collision integrals in only about 1 minute on our ICL 1907 computer to an accuracy of 1%. For an accuracy of 0.1% it takes about 3 minutes.

In the following we describe mainly the final methods we adopted in the program and say little about the many less efficient or less reliable methods we tried. These are discussed in more detail in a thesis by one of us [9].

1.1 Theory

The collision integral $\Omega^{(l,s)}(T)$ takes the form [2]

$$\Omega^{(l,s)}(T) = \frac{1}{2} \left(\frac{kT}{2\pi\mu} \right)^{\frac{1}{2}} \int_0^{\infty} e^{-x} x^{s+l-1} Q_l(kTx) dx \quad (1)$$

in which μ is the reduced mass of the two interacting systems and k is

Boltzmann's constant. In practice the integers l and s are small, usually less than 6. The collision cross section $Q_l(E)$ depends on the initial relative energy E and is given by

$$Q_l(E) = 2\pi \int_0^{\infty} b (1 - \cos^l \chi) db \quad (2)$$

where b is the impact parameter and χ is the classical deflection angle

$$\chi(b, E) = \pi - 2b \int_{r_m}^{\infty} \frac{dr/r^2}{[F(r, b, E)]^{1/2}} \quad (3)$$

in which r_m , the classical turning point, is the outermost zero of

$$F(r, b, E) = 1 - V(r)/E - b^2/r^2, \quad (4)$$

1.2 Difficulties

The problem thus reduces to the evaluation of the triple integral represented by equations (1) to (3). Difficulties arise because of certain singularities on or near the interval of integration in equations (2) and (3) which we will discuss later. Therefore our main difficulty is the calculation of the cross sections $Q_l(E)$. The evaluation of the integral in equation (1) is relatively easy.

Fortunately we can make one immediate simplification by noting that $Q_l(E)$ is a single-valued function of the single real variable E for each value of l . Thus $Q_l(E)$ can be determined at a discrete set of energies E_i and further cross sections found quickly by interpolation in the first set. It is not therefore necessary to calculate a

new set of cross sections, $Q_{\mu}(E)$, for each temperature, T . The problem is now reduced to: (a) the evaluation of a set of awkward double integrals represented by equations (2) and (3); (b) choosing the energies E at which these cross sections are best evaluated; (c) interpolating in these cross sections and (d) evaluating a set of simple integrals represented by Equation (1).

We add a condition to all our numerical processes: the program reads in a permitted relative error or accuracy ϵ , the final collision integrals must be correct to this accuracy. Also, as far as possible the amount of computation should be minimized to ensure the accuracy ϵ and no higher accuracy. Thus quick results to an accuracy 0.01 or necessarily longer calculations to an accuracy 0.0001 should both be possible. This means that we can only use numerical processes which allow us to estimate their accuracy reliably.

We begin by looking at the problem of the evaluation of a well behaved integral and of the integral in Equation (1). We next show how we remove the singularities in the double integral and we finally consider the problem of interpolation.

II Well Behaved Integrals

2.1 Clenshaw-Curtis method

We assume that we have reduced an integral by changes of variable to the form

$$I = \int_{-1}^{+1} F(t) dt \quad (5)$$

where $F(t)$ is well behaved in and near $(-1, +1)$. There are endless numbers of methods for evaluating such an integral but when we can choose the abscissas or pivots at any points in the interval including the end points and when we are asked to obtain an answer with a minimum number of function evaluations to an accuracy ϵ , then the choice is limited and one method stands out in front of the others, the Clenshaw-Curtis method [10, 11]. Because this method is not well known we will describe it briefly.

The integrand $F(t)$ is expanded in a finite Chebyshev series

$$F(t) = \sum_{r=0}^N a_r T_r(t) \quad (6)$$

where

$$a_r = \frac{2}{N} \sum_{s=0}^N \cos \frac{r\pi s}{N} F\left(\cos \frac{\pi s}{N}\right) \quad (7)$$

and the series is integrated term by term. A quadrature results

$$I_N = \sum_{s=0}^N h_s^N F\left(\cos \frac{\pi s}{N}\right) \quad (8)$$

where

$$h_s^N = (-1)^s \frac{2}{N^2-1} + \frac{4}{N} \sin \frac{\pi s}{N} \sum_{i=1}^{\frac{1}{2}N} \frac{\sin [(2i-1)\pi s/N]}{2i-1}$$

for $1 \leq s \leq N-1$,

(9)

$$h_0^N = h_N^N = (N^2-1)^{-1}$$

These weights are easily computed at the beginning of the program for any N needed.

The quadrature in Equation (8) has several advantages. It is extremely accurate (nearly as accurate as Gaussian quadratures) partly because a Chebyshev series converges so quickly and partly because it can be shown [11] that not only are the contributions to the integral from the harmonics $r = 0$ to $r = N$ in Equation (6) evaluated, but most of the contribution to the integral from the higher harmonics^c between $N + 1$ and $2N - 1$ are also included. Hence the ~~accuracy~~^{precision} is nearly that of a Gaussian quadrature, $2N - 1$. But the method has a number of advantages over Gaussian quadratures. First of all, the function evaluations in the 9-point quadrature ($N = 8$) are common with the 17-point quadrature ($N = 16$). So we can double the number of points without losing function evaluations (as in Simpson's rule). An even bigger advantage is the range of possible error estimates [11].

Of these we adopted the estimate

$$E_N = \frac{16N}{(N^2-1)(N^2-9)} \text{maximum} \left\{ |a_N|, \frac{1}{2}|a_{N-2}|, \frac{1}{8}|a_{N-4}| \right\} \quad (10)$$

where

$$a_{N-2r} = \frac{2}{N} \sum_{s=0}^N (-1)^s F\left(\cos \frac{\pi s}{N}\right) \cos \frac{2\pi r s}{N}$$

This is easily computed since it depends only on the function evaluations needed in the quadrature. Since it is the maximum of three quantities the possibility of one or two of them being accidentally very small is ruled out. It is shown in [11] that E_N is reliable provided

$$|a_N| < \frac{1}{2} |a_{N-2}| < \frac{1}{8} |a_{N-4}|$$

When this test failed we continued the calculation till E_N was less than $\varepsilon/10$ rather than ε . This process rarely fails to give us an error bound, but for badly behaved integrals where experience shows it does fail we use in place of E_N the "conservative" error estimate

$|I_N - I_{N/2}|$. In the end we were able to ensure by appropriate changes of variable that none of our integrals ^{was} ~~were~~ this badly behaved.

Because of the lack of similar error estimates in Gaussian quadratures the Clenshaw-Curtis method is preferred. Other quadratures such as Romberg's algorithm are too inefficient to be comparable to the Clenshaw-Curtis method for our purposes. A recent variation on Gaussian quadratures due to Patterson [12] is the nearest competitor to the Clenshaw-Curtis method, but we think that it, too, falls down because of the lack of a sufficiently good error estimate.

2.2 Infinite Intervals

The integrals in Equations (1) to (3) are over an infinite range. To put them in the form where we can use the Clenshaw-Curtis formula we must change the variable. We illustrate a difficulty by writing Equation (1) in the form

$$\Omega^{(l,s)} = \int_0^{\infty} g(x) dx \quad (11)$$

One possible change of variable is given by

$$\alpha x = (1-t)/(1+t) \quad (12)$$

For any α this changes the integral in Equation (11) into the form in Equation (5), but the efficiency of the resulting quadrature will vary greatly with different values of α . For example, for very large α a sharp peak will appear near $t = -1$, and for very small α a peak appears near $t = +1$. The choice of the correct α presents a difficulty, but fortunately we can often use some analytic information to determine α as we now show.

2.3 The Integral in Equation (1)

In the case of Equation (1) the integrand typically takes the form shown in Fig. 1. Because $Q_\ell(E)$ varies slowly with E the shape of this integrand is dominated by the term $(e^{-x} x^{s+1})$ which has a peak at $s+1$. We therefore use $x = s+1$ as an approximation to the position of the peak in the integrand. We split the integral in two parts at $s+1$ and integrate the second part by changing the variable to $y = (s+1)/x$ (effectively we are allowing the position of the peak to determine the α parameter for us):

$$\Omega^{(\alpha, s)}(T) = \int_0^{s+1} e^{-x} x^{s+1} Q_\ell(kTx) dx + (s+1) \int_0^1 \frac{e^{-x} x^{s+1} Q_\ell(kTx) dy}{y^2} \quad (13)$$

The first \int_0^{s+1} integral is now readily put in the form of Equation (5) by a linear transformation.

Because of the e^{-x} term we know that the integrand and all of its derivatives are zero at $y = 0$; thus the reflection of the integrand into the interval $(-1, 0)$ produces a smooth even function over the whole interval $(-1, +1)$. We can use this information by adopting only the positive Clenshaw-Curtis abscissas and the corresponding weights in the evaluation of this second integral.

Note that since the abscissas in the Clenshaw-Curtis quadrature are concentrated near the ends of the range, the above changes of variable have effectively concentrated the abscissas mainly in the region of the maximum in the integrand.

The accuracy of these methods is demonstrated in Table 1 for the two integrals in Equation (13). A number of other changes of variable ~~was~~ ~~were~~ tried but as expected these were not as accurate as the above.

III Cross Sections for a Repulsive Potential

3.1 Cross Section Integral

The calculation of the cross section $Q_{\ell}(E)$ by evaluating the double integral in Equations (2) and (3) is straightforward when the intermolecular potential is repulsive for all values of r . Then the angle χ falls monotonically from π to zero as b increases from zero to infinity. There is then only one maximum in the integrand $b(1 - \cos^2 \chi)$ in Equation (2) near the impact parameter b' at which $\chi = \frac{1}{2}\pi$. We therefore compute b' approximately by scanning χ at different values of b and using the fact that b' decreases as the energy E increases to start us on each scan. On average b' is computed approximately after only 4 or 5 calculations of the angle χ .

Once we have found b' we use the method in (2.3) to evaluate the integral - with one difference. In the integral from b' to infinity we could have used the positive abscissas as we do in (2.3). However, this concentrates the abscissas near b' with few abscissas at large values of b . This is ideal for the integrand in Equation (13) because of its decreasing exponential term but in the integral in Equation (2), particularly when the potential falls to zero slowly as r increases to infinity, a large part of the integral comes from large b values. Therefore, we adopted the change of variable

$$y = z(b'/b) - 1 \quad (14)$$

and the integral becomes

$$\int_0^{\infty} b(1 - \cos^l \chi) db = \int_0^{b'} b(1 - \cos^l \chi) db + \frac{1}{2b'} \int_{-1}^{+1} b^3 (1 - \cos^l \chi) dy. \quad (15)$$

Clenshaw-Curtis quadratures are used on both integrals once the range in the first integral is changed to $(-1, +1)$. The abscissas are now concentrated near b' and they extend to large values of b .

This method has proved to be efficient and reliable. Often only 9 abscissas are needed to ensure the evaluation of each integral to an accuracy of 1 in 1000.

3.2 The Angle Integral

The calculation of the deflection angle χ is also relatively straightforward for a repulsive potential. The pole at r_m , the classical turning point, in the integrand in Equation (3) can be eliminated by Gauss-Mehler quadratures [13] or by a change of variable such as

$$\cos\left[\frac{1}{4}\pi(x+1)\right] = r_m/r \quad [14]. \quad \text{Then Equation (3) becomes}$$

$$\chi(b, E) = \pi \left[1 - \frac{b}{2r_m} \int_{-1}^{+1} \frac{\sin\left[\frac{1}{4}\pi(x+1)\right] dx}{\left\{F(r_m/\cos\frac{1}{4}\pi(x+1), b, E)\right\}^{\frac{1}{2}}} \right] \quad (16)$$

This quadrature converges a little less slowly than the Gauss-Mehler quadrature but it is still preferable because of the difficulty of finding a good error estimate in the Gauss-Mehler method. Also because the abscissas in successive Gauss-Mehler quadratures do not overlap we lose all our previous function evaluations each time we change the order of the quadrature.

3.3 The Classical Turning Point

The classical turning point r_m can be found by inverse interpolation [6] for any impact parameter b . Because the integrand in Equation (3) is infinite at r_m it is important that we calculate r_m very accurately. We therefore adopt the following process: we begin with the given value of b , we calculate an approximate r_m , we recalculate a new b from the precise formula

$$b'' = r_m \left(1 - V(r_m)/E \right)^{\frac{1}{2}} \quad (17)$$

and then we calculate $\chi(b'', E)$ rather than $\chi(b, E)$. Small errors in r_m will result in a small difference between b and b'' and a resulting small difference between $\chi(b'', E)$ and $\chi(b, E)$, much smaller than the error obtained by using the slightly incorrect r_m and the correct b in Equation (14). The necessity for calculating r_m accurately is demonstrated in Fig. (2) by the large slope of $F(r, b, E)$ at $r = r_m$. This term is in the denominator of the integral from which we calculate the angle χ .

IV Cross Sections at Orbiting Energies

When the interatomic potential has a minimum the cross sections are much more difficult to calculate because of a phenomenon known as orbiting (the particles orbit about one another). Mathematically this occurs because of a non-integrable pole in the integrand in Equation (3) at what is called the orbiting impact parameter b_0 . This is illustrated in Fig. 2 where the term $F(r, b, E)$ in the denominator of the integral in Equation (3) is drawn ~~for different b values.~~ ^{for b near b_0 .} The curve corresponding to the impact parameter b_0 just touches the axis at $r = r_0$, so

$F(r, b_0, E)$ has a zero of order 2 at $r = r_0$, the integrand in Equation (3) has a pole of order 1 and $\chi = -\infty$. The integrand $b(1 - \cos^2 \chi)$ then has an infinite number of oscillations in the region of b_0 .

The orbiting phenomenon illustrated in Fig. 2 only occurs at low energies: when E is large the term $V(r)/E$ is small compared with b^2/r^2 and the slope of $F(r, b, E)$ is always positive as it crosses the axis. There is a critical energy E_c below which orbiting occurs and above which it cannot occur, but at energies just above E_c there are still a lot of oscillations in the integrand, $b(1 - \cos^2 \chi)$ in Equation (2) although there is no singularity. Thus we find that we have to consider three energy regions separately:- 1. energies below E_c ; 2. energies just above E_c (which we took to be E_c to $10 E_c$); and 3. energies well above E_c .

4.1 Region 1, $E < E_c$

4.1.1 The Angle

When orbiting occurs both the integral for the angle and the integral for the cross section give us trouble. The integral for χ in Equation

(3) is particularly difficult for b less than, but close to b_0 . By examining Fig. 2 it is apparent that the integrand has a ~~sharp~~ peak near r_0 as well as a pole at r_m . This ~~sharp~~ peak makes the simple method described for the repulsive potential converge slowly. Because the abscissas in the Clenshaw-Curtis method are concentrated near the ends of the range we split the integral in Equation (16) at the value $x = x_0$ corresponding to $r = r_0$. The peak occurs somewhere near x_0 . Then $\chi(b, E)$ becomes

$$\chi(b, E) = \pi \left\{ 1 - \frac{b}{2r_m} \int_{-1}^{x_0} + \int_{x_0}^1 \frac{\sin \left[\frac{1}{4} \pi (x+1) \right] dx}{\left[F \left(r_m / \cos \frac{1}{4} \pi (x+1), b, E \right) \right]^{\frac{1}{2}}} \right\} \quad (18)$$

In the first integral we introduce the change $x = (x_0 + 1) \cos \theta$ to concentrate the pivots near the peak at x_0 . A similar change is introduced into the second integral. Both of the resulting integrals are now put in the form in Equation (5) by linear variable changes and evaluated by Clenshaw-Curtis quadratures. In Table 2 the efficiency of this method is compared with the method in Equation (16) for a value of b less than and close to b_0 . Clearly this is a case when splitting the integral pays dividends. We adopt this method for all $b < b_0$. For $b > b_0$ there is no difficulty and the method described earlier for a repulsive potential is used.

4.1.2 The Cross Section

The integral for the cross section in Equation (2) is even more difficult. Because χ diverges at b_0 the integrand has an infinite number of oscillations near b_0 . This is illustrated in Fig. 3. We break the integral into two parts at b_0 . In the integral from 0 to b_0 we note that the integrand is largest and it varies most quickly near b_0 .

In addition at b_0 we cannot calculate the integrand. We therefore seek a change of variable that concentrates the abscissas near b_0 and such that the new integrand is zero at the end corresponding to b_0 . One (of many) such changes of variable is $b = b_0 \cos[\frac{1}{4}\pi(x+1)]$.

So

$$\int_0^{b_0} b(1 - \cos^l \chi) db = \frac{1}{8}\pi b_0^2 \int_{-1}^{+1} \sin[\frac{1}{2}\pi(x+1)](1 - \cos^l \chi) dx \quad (19)$$

The singularity is now at $\chi = -1$ where the integrand is zero. Thus the singularity is effectively eliminated. This change of variable works extremely well and transforms an almost impossible integral into one which we can readily and quickly evaluate. Typically we obtain three figure accuracy with 17 Clenshaw-Curtis quadrature points.

In the case of the integral from b_0 to infinity we note that if we change the variable from b to r_m then since $\frac{db}{dr_m} = 0$ at $b = b_0$, the new integrand is also zero at b_0 and we have eliminated the singularity [3] :

$$\int_{b_0}^{\infty} b(1 - \cos^l \chi) db = \int_{r_0}^{\infty} r_m \left[1 - \frac{V(r_m)}{E} - \frac{r_m V'(r_m)}{2E} \right] (1 - \cos^l \chi) dr_m \quad (20)$$

The difficulty with this change of variable is that it introduces the derivative of the potential, often not easily calculated. For this reason we did not adopt this change of variable generally. We adopted ~~this~~ ^{it} ~~change of variable~~ partly for historical reasons, ~~though~~ ^{though} Other variable changes would have given as good results; for example the change leading to Equation (19) .

The new integral in Equation (20) can now be evaluated by changing the variable so that the interval is $(-1, +1)$, e.g.

$$r_m = 2r_0 / (\kappa + 1). \quad (21)$$

But we found that χ falls to zero so quickly as b increases that the integrand is still concentrated near the end point $\kappa = +1$. We therefore made yet another change of variable to concentrate the abscissas even closer to b_0

$$r_m = r_0 / \sin(\frac{1}{2}\pi y) \quad (22)$$

So as

$$\int_{b_0}^{\infty} b(1 - \cos^2 \chi) db = \frac{1}{2}\pi \int_0^1 r_m \left[1 - \frac{V(r_m)}{E} - \frac{r_m V'(r_m)}{2E} \right] \frac{1 - \cos^2 \chi}{\sin^2 \frac{1}{2}\pi y} \cos \frac{1}{2}\pi y dy \quad (23)$$

The integrand and all of its derivatives are zero at $y = 0$ so we can use only the positive Clenshaw-Curtis points in the quadrature. This proved to be the most successful of a number of methods tried. We typically obtained an accuracy of 0.1% or less with only 17 abscissas.

4.2 Region 2, $E_c < E < 10E_c$

For energies just above the critical energy E_c the angle χ remains finite and no orbiting occurs. However, χ does fall to a negative minimum value (the rainbow angle) and the integrand $b(1 - \cos^2 \chi)$ has a number of oscillations in the region of this minimum; the closer E is to E_c the more oscillations there are. In the program we find the

approximate position of the minimum angle, $b = b_r$, quickly by scanning χ at different b and using the information that b_r decreases as E increases and that b_r is less than b_0 at E_c . Since most of the oscillations occur near b_r and since we therefore wish to concentrate our abscissas near b_r we break the integral into two parts at b_r .

The integral from b_r to infinity we evaluate in the same way as we evaluated the equivalent integral in (4.1.2) with b_0 replaced by b_r . In this $\frac{db}{dr_m}$ is no longer zero, but it is small at b_r and the transformation from b to r_m is still advantageous. For the same reason it can also be used with advantage in the first part of the integral from 0 to b_r , and indeed we found this the most efficient method of evaluating this integral. Thus our whole integral becomes

$$\int_0^{\infty} b (1 - \cos^2 \chi) db = \int_{r_{m0}}^{r_{m1}} b \frac{db}{dr_m} (1 - \cos^2 \chi) dr_m + \frac{1}{2} \pi \int_0^1 b \frac{db}{dr_m} \frac{(1 - \cos^2 \chi)}{\sin^2 \frac{1}{2} \pi y} \cos \frac{1}{2} \pi y dy \quad (24)$$

in which r_{m0} and r_{m1} are the turning points corresponding to $b = 0$ and $b = b_r$ respectively, y is defined by Equation (22) with r_0 replaced by r_m and

$$b \frac{db}{dr_m} = r_m \left[1 - V(r_m)/E - r_m V'(r_m)/(2E) \right] \quad (25)$$

A simple linear change of variable puts the first integral in the form of Equation (5) for the Clenshaw-Curtis quadrature and the second integral uses only the positive abscissas.

The angle χ is readily computed in all cases by the method used for the repulsive potential in (3.2).

4.3 Region 3, $E < 10E_c$

Well above the critical energy the minimum (rainbow) angle is small and there are just two bumps in the integrand $b(1 - \cos^2 \chi)$, one when χ is near $\frac{1}{2}\pi$ as for the repulsive potential and the second at the minimum angle. At very large energies ($E > 1000 E_c$) the contribution from this second bump is small and we use the same routines as we have described for the repulsive potential in (3.1) which concentrate the abscissas near the first bump only.

delete (c) At intermediate energies ($10E_c < E < 1000E_c$) we split the integrand at b_2 (which we note is nearly equal to r_0 at $E = E_c$ in all cases) and then adopt the same routines as we use for the repulsive potential with b' replaced by b_r .

V Interpolation

As we have explained in our introduction the most efficient way of calculating a set of collision integrals $\Omega^{(a,s)}(T)$ for different temperatures T is to calculate an initial set of cross sections $Q_\ell(E_i)$ and interpolate for the many further cross sections needed. The range over which the energies E_i must be chosen is between E_{\min} and E_{\max} :

$$E_{\min} = k T_{\min} \chi_{\min} \quad ; \quad E_{\max} = k T_{\max} \chi_{\max} \quad (26)$$

where T_{\min} and T_{\max} are the minimum and maximum temperatures and χ_{\min} and χ_{\max} are the minimum and maximum abscissas needed to evaluate the integral in Equation (1). Usually E_{\max} is many orders of magnitude larger than E_{\min} so this calls for a logarithmic scale in our choice of energies. Further, plots of $\text{Log} [Q_\ell(E)]$ against $\text{Log} E$ are much smoother functions of $\text{Log} E$ than are plots of $Q_\ell(E)$ against $\text{Log} E$. Not surprising then is our discovery that interpolation in tables of $\text{Log} [Q_\ell(E)]$ gives better results than in tables of $Q_\ell(E)$. We illustrate the smoothness of $\text{Log} [Q_\ell(E)]$ against $\text{Log} (E)$ in Fig. 4.

Fig. 4 also shows that the plots of $\text{Log} [Q_\ell(E)]$ fall into the three regions we mentioned in the last section: Region (1): $E < E_c$, Region 2: $E_c < E < 10E_c$, Region 3: $10E_c < E$. We curve fitted or interpolated in these three regions separately.

There were three different methods available for the interpolation

- (a) Lagrangian (Aitken's) method
- (b) Cubic Splines [15]
- (c) Polynomial curve fitting

Method (b) we found gave slightly more accurate answers than piecewise cubic Lagrangian interpolation, but less accurate answers than, say, quintic Lagrangian interpolation. It also used more storage space since the second derivative at each pivot must be stored. Its biggest drawback is the lack of a facility for estimating the error realistically and in our case this is essential since we wish to double the number of energies in our table in successive ^{steps} ~~strips~~ until we can interpolate to the accuracy we require. For this purpose Lagrangian interpolation is better because we can examine the interpolates obtained using parabolic, cubic, quartic, etc. fits to adjacent points and use these to estimate the error at a number of energies chosen at random in the range. But there are still inaccuracies especially at the ends of the range.

The third choice is a polynomial curve fit of all the points in the range. Here the position of the pivots in the range is crucial. Equidistant pivots give good answers in the middle of the range and poor answers (or divergent answers) at the ends of the range [16]. But if the range of integration is changed to $-1 \leq x \leq +1$ and the pivots chosen at the points

$$x_k = \cos(k\pi/N), \quad 0 \leq k \leq N \quad (27)$$

then the set of polynomials orthogonal over these pivots is the set of Chebyshev polynomials, $T_n(x)$. The resulting curve fit converges quickly as N increases and gives uniformly accurate results over the whole range.

We can determine this curve fit approximately as follows. We write

$$f(x) = \sum_{r=0}^N c_r T_r(x) \quad (28)$$

where the coefficients c_r are easily calculated from the relation

$$c_r = \frac{2}{N} \sum_{k=0}^N T_r(x_k) f(x_k) \quad (29)$$

Since $|T_r(x)| \leq 1$ and the Chebyshev series converges rapidly we can approximate the error by $|c_N| + |c_{N-1}|$ with some confidence.

In our case we are integrating over the functions which we are curve fitting and the contributions from the high order harmonics $T_N(x)$ will tend to cancel out because they oscillate considerably. Therefore, for our purposes we found empirically that it was sufficient to use as our error estimate

$$\epsilon_N = \frac{2}{N} [|a_N| + |a_{N-1}|]. \quad (30)$$

This method worked so well that we needed only 5 cross sections in Region 1, 9 in Region 2, and 5 in Region 3 to ensure that our interpolated collision integrals were correct to 1%. A typical set of coefficients are given in Table 3.

VI Conclusion

We have described how we optimised each step in our calculations. The resulting program is extremely efficient. The times needed to calculate for a Lennard-Jones (6-12) potential a complete set of cross sections $1 \leq l \leq 6$ or a set of collision integrals $1 \leq l, s \leq 6$ at 40 different temperatures is given in Table 4 for different required accuracies ϵ . The actual errors were less than the tolerated errors in all cases we tested.

We have checked the program by running it for the 12-6-3 and 12-6-5 potentials for which results are available [4, 17] and for the potential e^{-r}/r . The program of Smith and Munn [6], probably the best previous general program, gave incorrect results for this last potential at high temperatures [7, 8]. Our program gave the correct results but it also sent out an error message warning that the results were not entirely reliable at high temperatures. In this case the potential effectively falls off very slowly at high energies and this severely tests any transport program. We were pleased that our program dealt with it so well.

We are reasonably convinced that the efficiency and reliability of our program cannot be greatly improved.

REFERENCES

1. S. Chapman and T.G. Cowling, "The Mathematical Theory of Non-Uniform Gases", 2nd Ed., Cambridge University Press, New York, (1952).
2. J. O. Hirschfelder, D. F. Curtiss and R. B. Bird, "Molecular Theory of Gases and Liquids", Wiley and Sons, Inc., New York (1954).
3. E. A. Mason, J. Chem. Phys. 22; 169-186 (1954).
4. L. Monchick and E. A. Mason, J. Chem. Phys. 35, 1676 - 1697. (1961).
5. J. A. Barker, W. Fock and F. Smith, Phys. Fluids 7, 897-903, (1964).
6. F. J. Smith and R. J. Munn, J. Chem. Phys. 41, 3560-8, (1964).
7. R.J. Munn, E. A. Mason and F. J. Smith, Phys. Fluids 8, 1103-4, (1965)
8. E. A. Mason, R. J. Munn and F. J. Smith, Phys. Fluids 10, 1827-32, (1967).
9. H. O'Hara, Thesis, The Queen's University of Belfast, N. Ireland (1969).
10. C. W. Clenshaw and A. R. Curtis, Num. Math. 2, 197-205, (1960).
11. H. O'Hara and F. J. Smith, Comp. J. 11, 213-9, (1968).
12. T. N. L. Paterson, Maths. Comp. 22, 847-56, (1968).
13. F. J. Smith, Physica 30, 497-504, (1964).
14. T. Kihara and M. Kotani, Proc. Phys. Soc. - Math. Soc. (Japan) 25, 602 -
(1943).
15. B. Wendroff, "Theoretical Numerical Analysis", Chapter 1., Academic Press, New York, (1966).
16. C. Lanczos, "Applied Analysis", Chapter 5, Prentice Hall, New Jersey (1956)
17. F. J. Smith, R. J. Munn and E. A. Mason, J. Chem. Phys. 46, 317-21, (1967).

Table 1.

Errors in quadratures evaluating the integrals in Eqn. (13) for the Lennard-Jones 6-12 potential where n is the number of intervals.

n	Error	n	Error
8	0.0011	4	0.2394
16	0.0008	8	0.0103
32	0.0001	16	0.0004
Integral	10.2165	Integral	12.4853

Table 2.

A comparison of the errors in two methods of evaluating the angle χ at a value of b close to b_0 for the (6-12) potential. In method (1) the integral is evaluated in the same way as for a repulsive potential without splitting the integral into two parts. In method (2) the integral is split near $r=r_0$. Here $E=0.23E_0$ and $b=0.991b_0$. n is the number of abscissas.

n	Method 1	Method 2
9	0.24369	-
17	0.01922	0.00074
33	0.01059	0.00005
65	0.00015	0.00000

Table 3

A typical set of Chebyshev coefficients fitting $\ln(Q_1(E))$, against $\ln(E)$ in the three energy regions. These are for the 6-12 potential with $\epsilon = 1\%$.

	Coefficients		
	Region 1	Region 2	Region 3
C_0	7.5353	3.0050	0.2521
C_1	-1.6523	-0.5599	-0.9061
C_2	-0.0090	0.0837	-0.0064
C_3	-0.0070	0.0213	-0.0038
C_4	-0.0099	-0.0225	0.0058
C_5		0.0091	
C_6		-0.0015	
C_7		-0.0016	
C_8		0.0024	

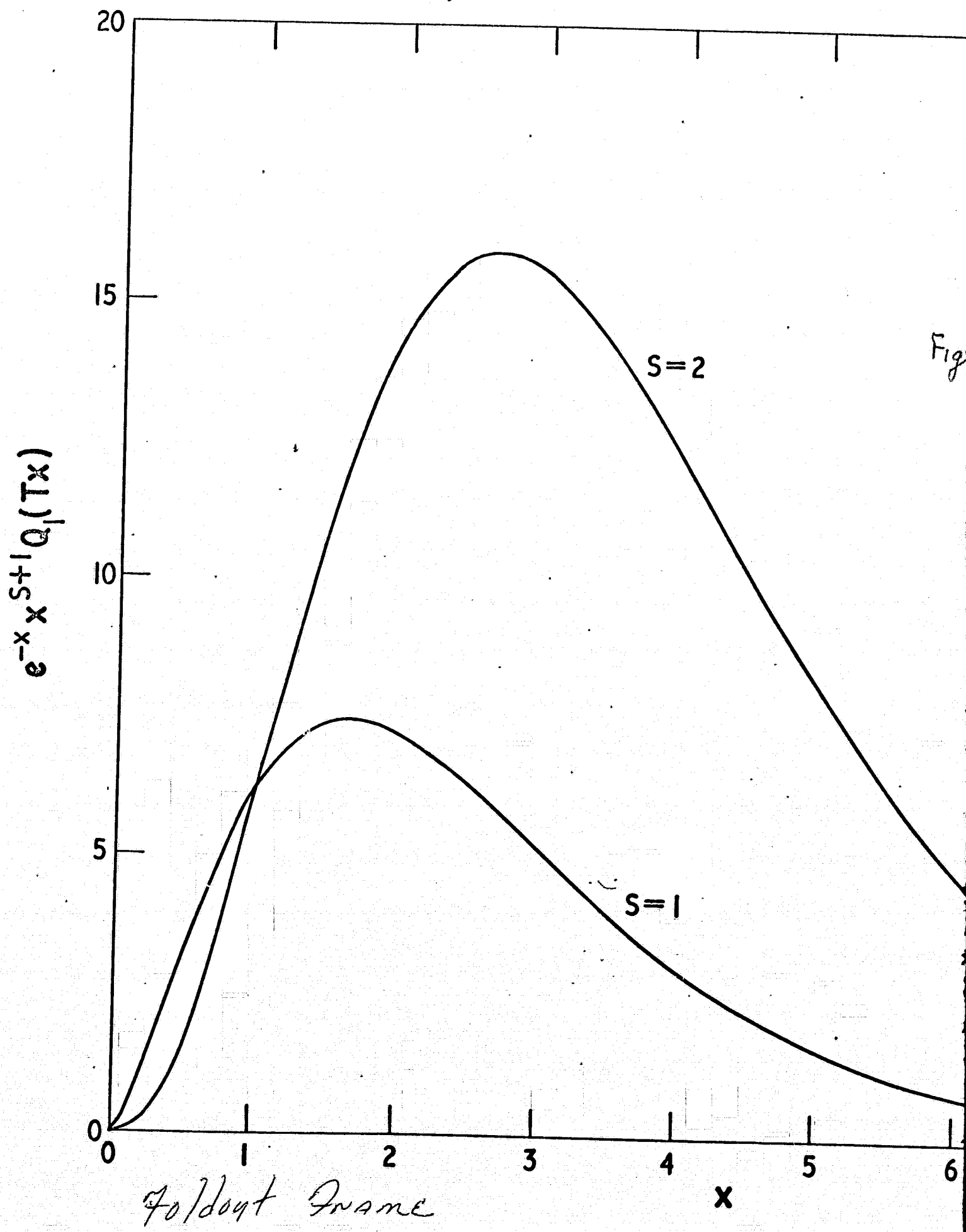
Table 4

A comparison of the times needed (a) to calculate a complete set of cross-sections $1 \leq l \leq 6$ and (b) to calculate a set of cross-sections and a complete set of collision integrals $1 \leq l, s \leq 6$ for 40 temperatures for different accuracies (ϵ). Also shown is the typical actual error obtained (err).

(ϵ)	0.01	0.001	0.0001	0.00001
(a)	1m.	2 $\frac{1}{2}$ m.	5 $\frac{1}{2}$ m.	20m.
(b)	2 $\frac{1}{2}$ m.	4 $\frac{1}{2}$ m.	10m.	29m.
(err)	0.002	0.0003	0.00003	-----

CHAPTER HEADINGS

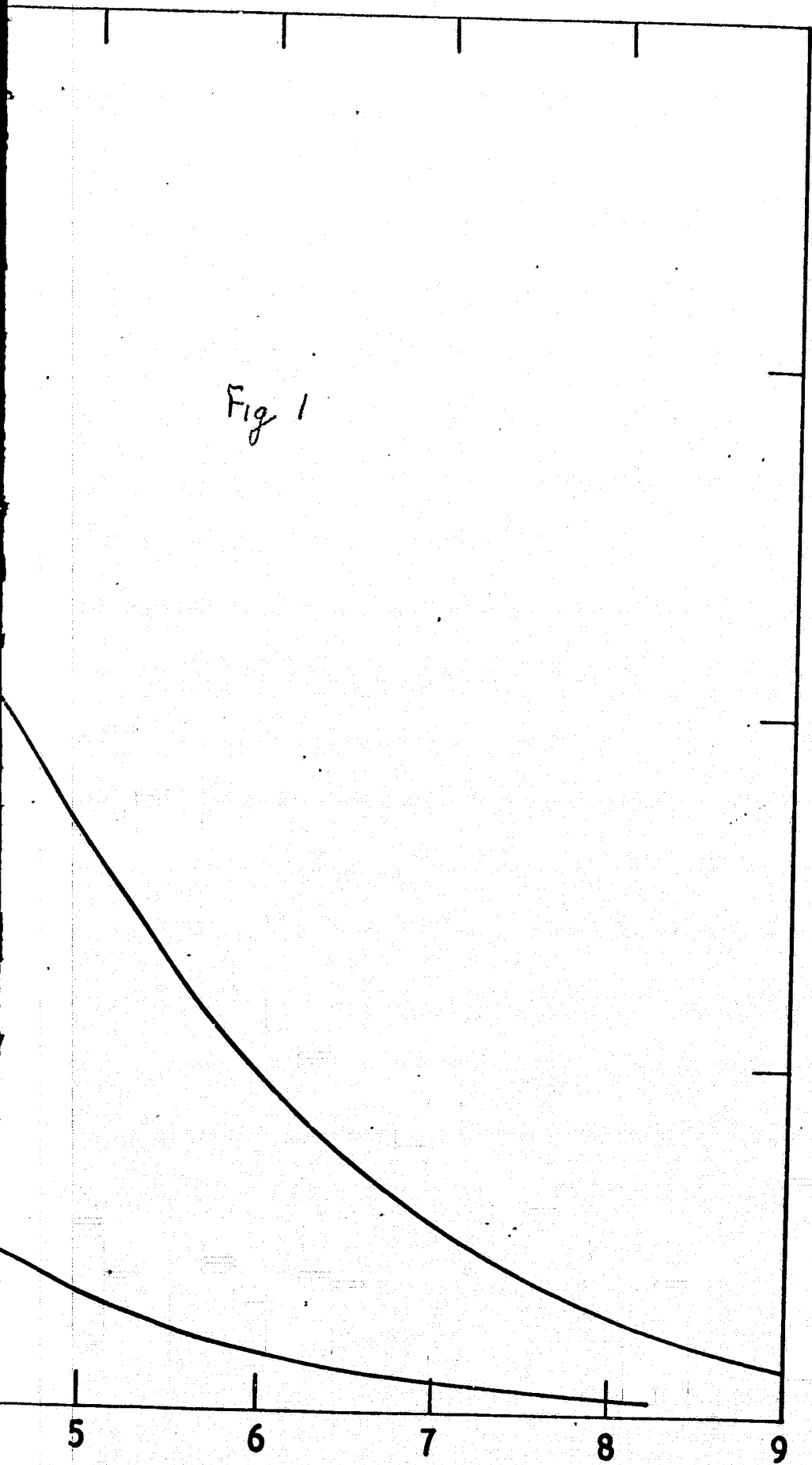
- FIG.1 The integrand in Eqn.(1) for the (12- ϵ) potential when $l=1$ and $T = 0.1/k$.
- FIG.2 The term $F(r,b,E)$ in the integrand in Eqn.(3) at a value of b near b_0 . Orbiting occurs at $b = b_0$ because $F(r,b_0,E)$ touches the axis at $r = r_0$. The integral in Eqn.(3) then diverges. For energies nearer E_c the shape would be similar but the maximum near r_m would be smaller. Here $E/E_c = \frac{1}{2} \cdot 10^{-5}$.
- FIG.3 The integrand, $b(1-\cos\alpha)$ in Eqn.(2) at an orbiting energy. There is an infinite oscillation at $b = b_0$.
- FIG.4 The cross-sections $Q_1(E)$ as a function of energy. This illustrates that a log-log plot is smooth and that there are three energy regions:-
 $E < E_c$; $E_c < E < 10E_c$; $10E_c < E$.



Fig

Foldout frame

Fig 1



70/dout frame
2

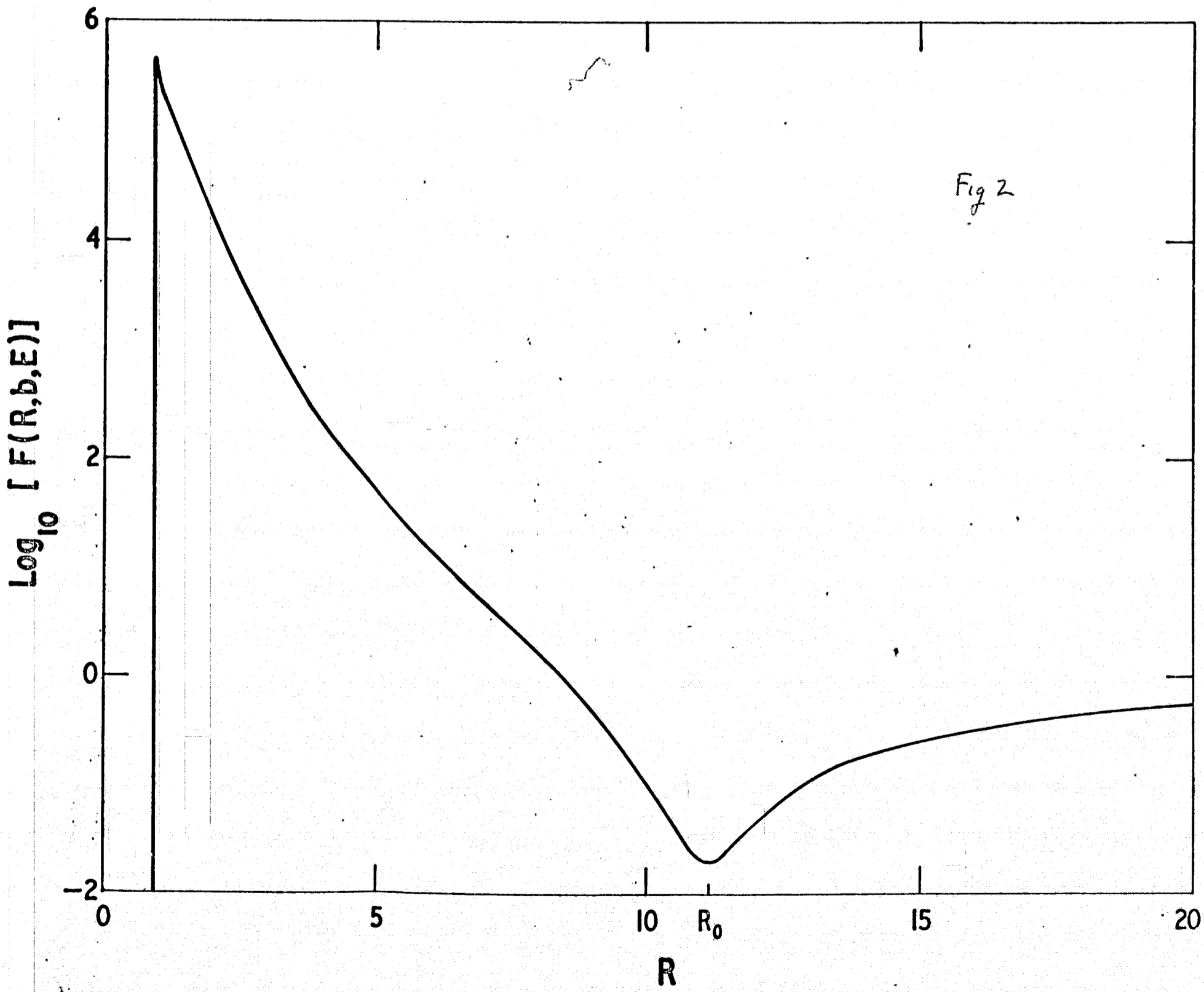
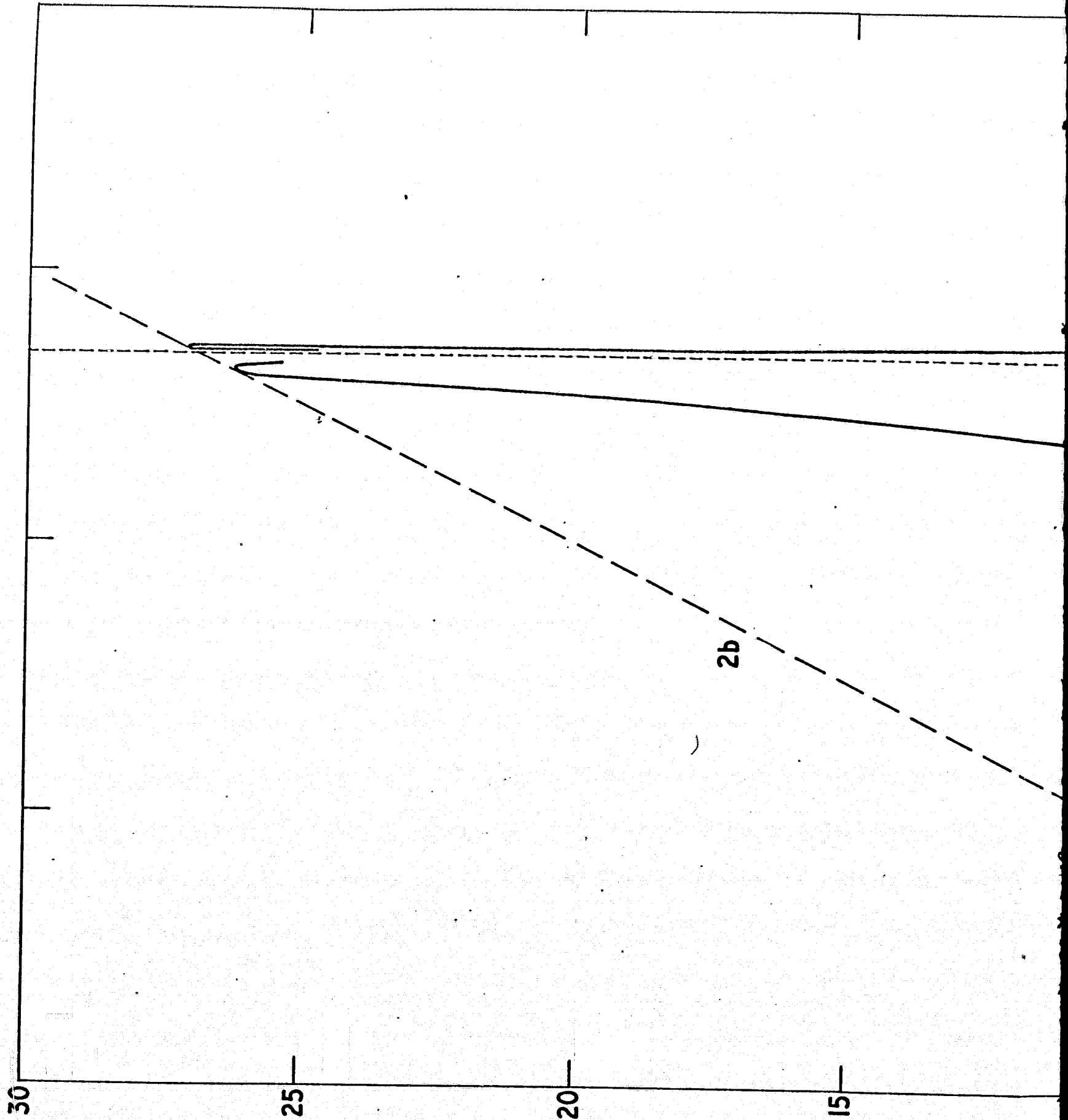
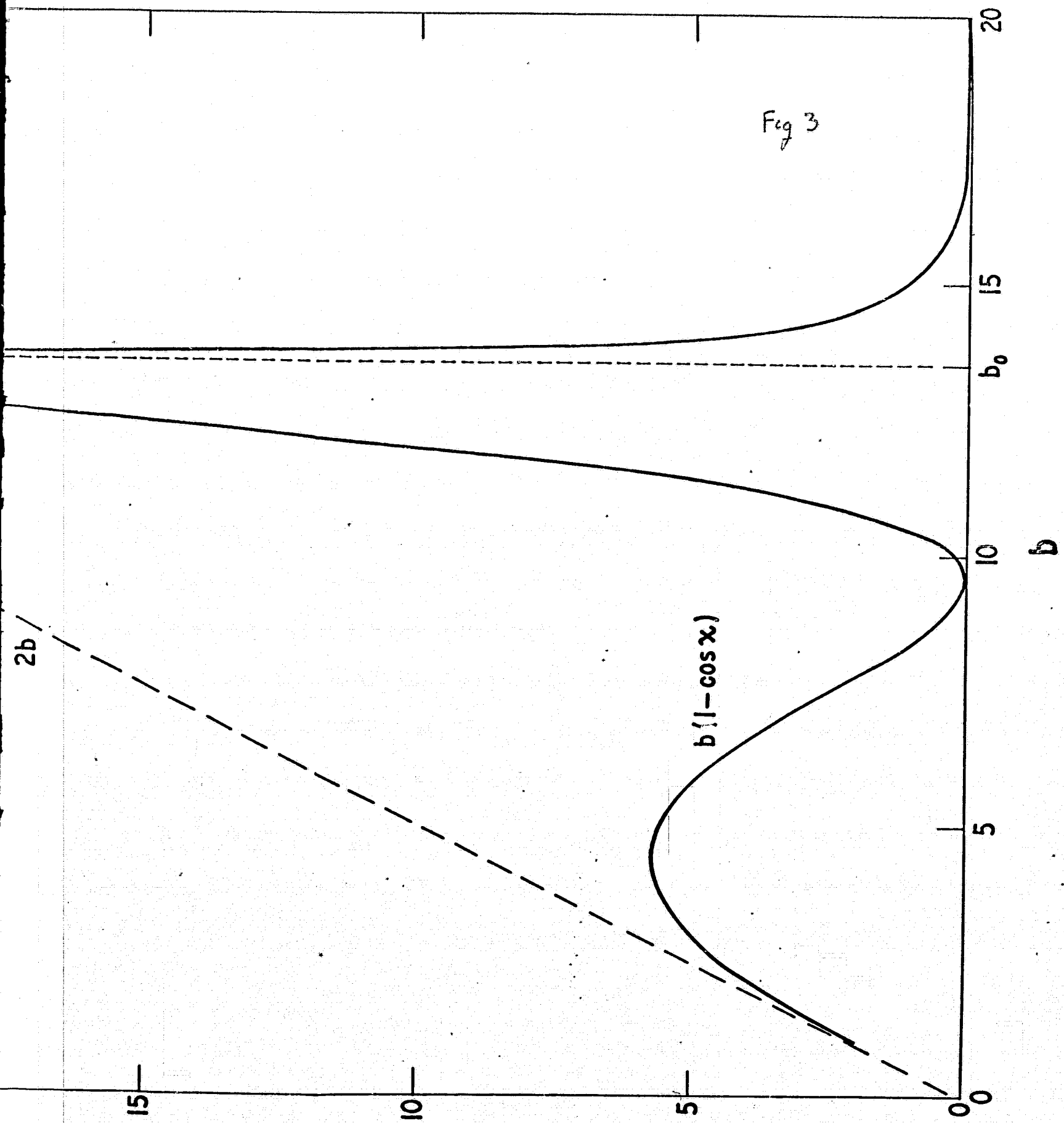


Fig 2

Fig 2



Foldout FRAME



foldout frame

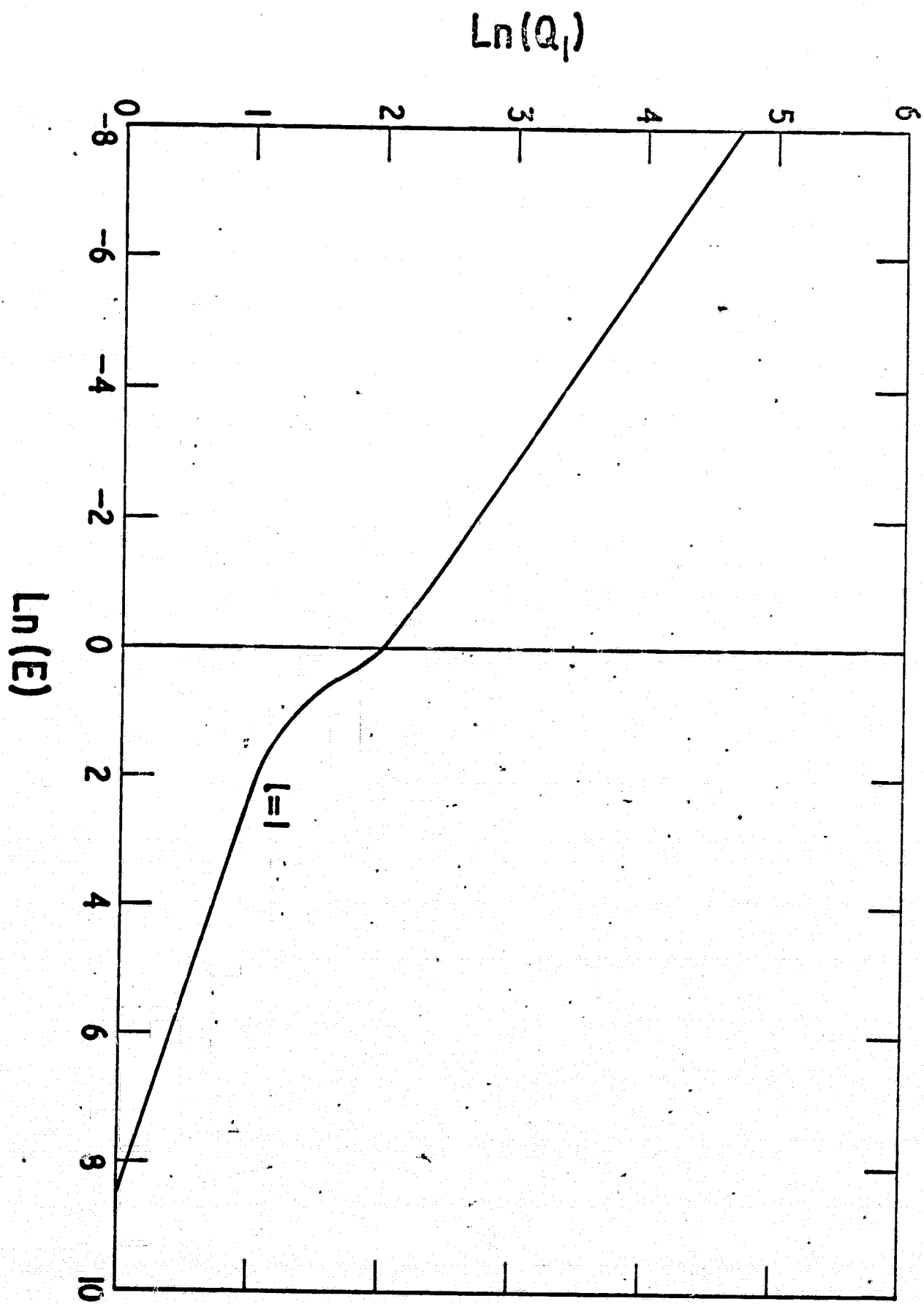


Fig 4